Design and simulation of a longitudinal autopilot system for flying vehicles based on LQR and Luenberger observer

M Ashraf[1], E Safwat[1], M A H Abozied[1] and A M Kamel[1]

[1] Missile Guidance Department, Military Technical College, Cairo, Egypt.

E-mail: mhmdashraf90@outlook.com

Abstract. A longitudinal autopilot system for flying vehicles, such as missiles and drones, is crucial for enhancing stability, reducing the risk of errors, improving efficiency, and providing better control in unpredictable situations. The advancement of such a system is imperative for advancing the aviation industry and ensuring successful missions carried out by these flying vehicles. The necessity for a reliable flight controller in agile missile applications motivates the design of this system. A state-space formulation was utilized to integrate a linear-quadratic regulator (LQR) method, a Luenberger observer, and proportional navigation algorithms. The design methodology aimed at minimizing a quadratic cost function while meeting performance objectives. The system was simulated using MATLAB, and the results demonstrate the autopilot's effectiveness in compensating for in-flight disturbances and noise caused by parametric uncertainties, environmental disturbances, and system non-linearities. The versatility of LQR optimization methods and the importance of robust control for stable and reliable missile systems in changing environments are emphasized in this observational study. Simulations and numerical analysis revealed a reduction in the miss distance, indicating the autopilot system's proficiency and robustness.

1. Introduction

An aerospace vehicle's longitudinal autopilot system is a crucial design step in accomplishing the terminal performance goals of eliminating a possible target. When agile missiles are used to engage a precise target, the task becomes significantly more challenging. Designing a multiple variables missile longitudinal autopilot for agile missile applications can be complicated due to various factors such as environmental variability, uncertain parameters, and system nonlinearity. A significant challenge is the lack of sensor data caused by defective signals and complete data loss in real flight, making feedback loops contesting. Given that inaccurate plant, and the sensor is noisy, these concerns become more significant, and the control system must cope with additional burdens. If the controller exceeds its limits, particularly in tactical missiles, it can cause design malfunctions and mission failure. An outstanding controller design for the missile's longitudinal dynamics can effectively compensate for in-flight disturbances and noise caused by scalar disturbances and Gaussian noise. This design technique allows the controller to integrate all disturbances during real flight, including internal noises and external system disturbances, and efficiently minimize a prescribed quadratic index [1]. Using the LQR method for controller design and incorporating the Linear-Quadratic Estimation (LQE) method to account for real flight disturbances, this study addressed a quadratic-cost function reduction problem while meeting

the desired performance objectives. The result was developing a system that produced optimal results with minimal effort required.

Aerospace vehicles experience various external perturbations and noise during real test flights, and if these factors are not considered, they can gradually propagate and cause system instability [2]. Several studies have been implemented to address this issue, and appreciable amount of relevant literature is available on this topic. In [3], LQR for stabilizing anti-aircraft pursuer's performance was analyzed. They proposed a new technique for selecting weighting factors in feedback loop's gain matrix, which was evaluated using the V-parameter-based method of LQR tuning. Additionally, in [4], the authors demonstrated the LQR applications in missile autopilot to control the roll angle of the system. They compared the results of LQR control with fuzzy logic control (FLC) and sliding mode control (SMC) using a second-order time-domain system to represent the rolling angle controllers. Authors in [5] used LQR to create a guidance law for tracking the target projectile's trajectory, with weight matrices optimized through an evolutionary algorithm to minimize the ITSE index and improve regulator efficiency. [6] Applies SMC to stabilize an anti-aircraft pursuer by decoupling the control process from the missile's airframe dynamics. The LQR method is employed in conjunction with an analytical approach to select the weighting components of the gain matrix.

Improved computer systems and numerical computation have facilitated the development of various LQR optimization techniques, enabling control of complex, multidimensional systems. LQR control has been successfully implemented in challenging applications, such as double-inverted pendulums, aircraft, and systems of fuel cell [7]. [8] Uses a combination of feed-forward and LQG feedback control to keep a ship model on a maneuvering trajectory, systematically selecting variances for the weighting coefficients of the LQG controller. Unlike fuzzy regulators or artificial neural networks, LQR requires a mathematical model of the system. However, LQR optimization techniques have been successful in various applications.

The authors in [9] utilized LQR to enhance the composite material production process through infusion. The study validated the potential for energy absorption with LQR in manufacturing composite materials using vacuum bagging. The focus is now on optimizing layer thickness selection to increase energy absorption. Furthermore [10], the author reviews most of LQR's techniques, which finally use it with the thrust vectoring control model of a missile. Top of Form

Bottom of Form

The selection of a control method for a system [11] begins with an analysis of the dynamic behavior of the plant. This involves understanding the rate of change of the system's state variables, which can be represented through a set of differential equations known as the flying object motion equations, which describe the relationship between the state variables and the fin deflections.

LQR is a modern control theory that analyzes the system's state space model, enabling state space techniques for complex systems. Control methods fall into two main categories: model-based, like LQG, which adopts a mathematical model, and model-less, like fuzzy regulators and artificial neural network-based control systems, which do not require a mathematical model. Motivated by the imperative to find a practical, reliable flight computer for applications involving agile missiles that will address this problem. The state-space formulation has been used in this study to conduct it inside a contemporary framework for control design.

This paper reveals a novel feedback control system design methodology to trace the vertical acceleration of a Medium-Range Air-to-Air Missile (MRAAM) and integrate it with a True Proportional Navigation Guidance Law. The methodology relies on robust servomechanism theory and Luenberger observer design and is divided into two parts. In the first one, the closed-loop system is designed with the required specifications using full-state feedback, then with acceleration and pitch rate as outputs. In the second part, the closed-loop system is integrated into the guidance law, and the minimum miss distance is evaluated, making any necessary changes to the design. To assist in the design process, design charts are created at crucial points.

The main contribution of this paper is the development of a systematic design process with detailed design charts, which aids in the implementation of the closed-loop system with the required specifications. This methodology is successfully applied to the MRAAM short-period dynamics, leading to an optimal realization of the missile's behavior and improved performance.
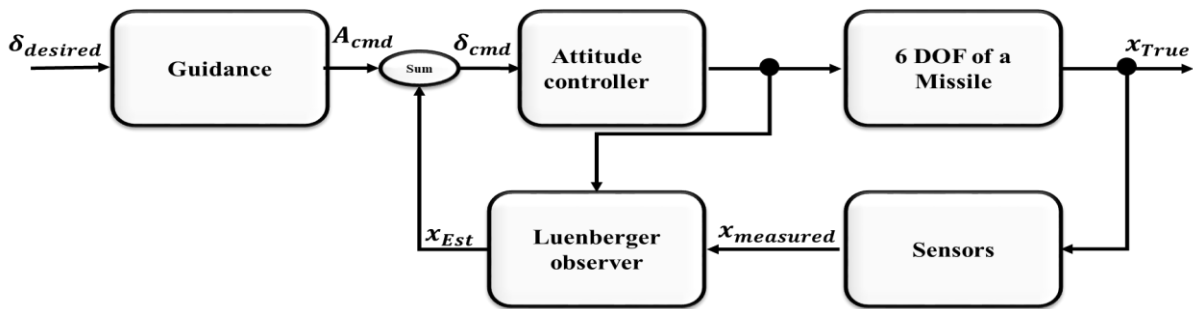
Figure 1. The proposed algorithm architecture design

Through extensive performance simulations, the paper demonstrates the potential of the design approach to handle the uncertain nature of the plant. Extensive performance simulations were conducted to evaluate the performance due to the plant's uncertain nature, validating the proposed approach's effectiveness.

This approach can be applied to other missile or aerospace systems with similar short-period dynamics. The structure of this paper is organized as follows: Section 2 presents the methodology for designing the missile control longitudinal autopilot, including the engagement dynamics and requirements. In Section 3, the design process is detailed with full-state feedback and observer design, and it is integrated with the guidance loop, in which the paper contribution is highlighted. Section 4 provides a simulation and analysis of the interception scenario. Finally, Section 5 concludes the work and provides directions and ideas for future areas of study.

2. Methodology

The conventional approach to guidance and control typically employs a hierarchical structure, where in guidance loop serves as the outer loop and is primarily responsible for generating the desired overload command. On the other hand, the control loop is responsible for tracking this overload command, ultimately achieving the missile's guidance toward its target. However, designing the control loop or autopilot with improved dynamic capability is often desirable. Despite this, practical limitations, such as delays and attenuations in the controller, can result in errors in following the overload command, contributing to a miss of the target.

To manage these issues, an integrated guidance and control algorithm has been developed that combines the guidance and control loops into a single loop, thus avoiding the delays and attenuations precipitated by their separation. The framework of this approach is illustrated in figure 1.

The states available for feedback include pitch rate and vertical acceleration (A_z). The actuator that provides inputs to the plant is a second-order under-damped system with unit steady state gain, albeit its dynamics are not characterized.

The control goal is to create an autopilot (controller and observer) that satisfies the problem statement's frequency and time domain requirements while ensuring that the closed-loop compensator's output (A_z) follows the intended ($A_{z_{cmd}}$). In addition, the last stage of (A_z) tracking ($A_{z_{cmd}}$) generated by the guidance issue must satisfy the actuator saturation requirements.

In order to decrease Miss Distance in the integrated autopilot-guidance system, all while fulfilling the other design requirements, the LQ Controller and Observer Penalty matrices must be tuned.

2.1. The Engagement Dynamics

The integrated guidance and control approach differs from other control methods in that it considers the dynamic attributes of the missile airframe. Thus, the derivation incorporates the missile's pitch angle, pitch rate, and angle of attack.

The missile's longitudinal motion is described by the following equations [12]:

$$\dot{V}_M = \frac{1}{m}(F_t \cos\alpha - F_x - m\,g\,\sin\theta_M) \tag{1}$$

$$\dot{\theta}_M = \frac{1}{m V_M}\left(F_t \sin\alpha + F_y - m\,g\,\cos\theta_M\right) \tag{2}$$

$$\dot{x}_M = V_M \cos\theta_M \tag{3}$$

$$\dot{y}_M = V_M \sin\theta_M \tag{4}$$

$$\dot{\omega}_{Z_M} = \frac{M_Z}{J_Z} \tag{5}$$

$$\dot{\theta} = \omega_Z \tag{6}$$

Where (x_M, y_M) is the missile position, m is the mass, F_x, F_y is the forces, F_t is the thrust force, the missile's velocity is (V_M), and its flight path angle is (θ_M), α is the attack angle and θ is the pitch angle.

The motion equations of the target are as follows:

$$\dot{x}_T = -V_T \cos\theta_T \tag{7}$$

$$\dot{y}_T = V_T \sin\theta_T \tag{8}$$

$$\dot{\theta}_T = \frac{a_{TN}}{V_T} \tag{9}$$

The interception of a target is described by two parameters: the target range and the line-of-sight (LOS) angle. The following relationships represent the kinematic equations associated with this process:

$$\dot{r} = -V_M \cos(\theta_M - q) - V_T \cos(\theta_T + q) \tag{10}$$

$$r\dot{q} = -V_M \sin(\theta_M - q) + V_T \sin(\theta_T + q) \tag{11}$$

Where (x_T, y_T) the target position, and LOS angle between the missile and its target is q, the relative range from the missile to its target is r, the velocity of the target is V_T, and its flight path angle is θ_T, $and\ g$ is the gravity force.

State-space equations represent the MIMO systems in contemporary control systems is;

$$\dot{X} = A\,X + BU$$
$$y = C\,X + DU \tag{12}$$

The vector of time derivatives of the state variables is $\dot{X}$, X is the vector of state variables, U is the vector of control inputs, the vector of outputs is y, and A, B, C, D is the state, input, output and the direct transmission matrices respectively.

Here, the longitudinal dynamics are linearized about the trim condition and represented in state_space form as given in the following,

$$\begin{bmatrix} \dot{u} \\ \dot{w} \\ \dot{q} \\ \dot{\theta} \end{bmatrix} = \begin{bmatrix} x_u & x_w & x_q & x_\theta \\ z_u & z_w & z_q & z_\theta \\ m_u & m_w & m_q & m_\theta \\ 0 & 0 & 1 & 0 \end{bmatrix} \begin{bmatrix} u \\ w \\ q \\ \theta \end{bmatrix} + \begin{bmatrix} x_{c\eta} \\ z_\eta \\ m_\eta \\ 0 \end{bmatrix} \delta_e \tag{13}$$

Where $[\dot{u}\ \dot{w}\ \dot{q}\ \dot{\theta}]^T$ represent the rates of change of the longitudinal state variables velocity, altitude, pitch rate, and pitch angle, respectively. $[u\ w\ q\ \theta]^T$ are the longitudinal state variables. The matrix elements $(x_i, z_i$ and $m_i)$, and i is $(u\ w\ q\ \theta)$ are the longitudinal stability derivatives, which represents the system dynamics. $[x_{c\eta}\ z_\eta\ m_\eta]^T$ represents the control derivatives, which relate the control input δ_e to changes in the state variables, and δ_e is the elevator deflection.

According to recent control theory, if the plant's system dynamics, i.e., matrices A and B, are controllable, the closed-loop system's eigenvalues can be manipulated. $[A - BK_r]$ by selecting the formulation of full-state feedback controller $u = -K_r x$. This method assume that the full state measurements to be available, i.e., $C = I$ and $D = 0$, in which $y = x$. The issue occurs as the system dimension develops and full-state controllability and observability become more challenging to implement. The sensor measurement data can be used to create a full-state estimation if the system is observable [13].

2.2. The Controller Requirements

The design requirements for the control system are as follows: the compensator must provide a minimum gain of 6 dB, ensuring that the system has enough amplification to meet the desired

performance specifications. A phase margin of 35 degrees guarantees that the system is stable and does not oscillate excessively. The maximum fin displacement and rate were also constrained to 35 degrees and 350 degrees per second, respectively, vouching that the system operates within the physical limits of the hardware. Then, the loop gain at the input crossover frequency was required to be less than One-third of the actuator's natural frequency to maintain that the actuator could keep up with the system's dynamics and not become a limiting factor, and the percentage undershoot and overshoot is both limited to 10 percent.

The sensitivity and co-sensitivity of the compensator were required to be less than 6 dB over the frequency range of 1e-1 to 1e3 rad/s, ensuring that the compensator does not introduce excessive noise or distortion in the system, as in figures 3 and 4. Furthermore, the real part of the closed-loop compensator eigenvalues had to be greater than -400 to know that the system is stable and has a fast response. Finally, the compensating loop gain had to be within 0.3 Hz of the LQR loop gain at the model, maintaining the input so the control system could track the desired trajectory accurately. These requirements were used as the basis for the simulation and evaluation of the control system.

3. Autopilot Design

While adhering to the design specifications, the LQ Controller and Observer Penalty matrices must be optimized to reduce Miss Distance in the integrated autopilot-guidance system. Despite plant uncertainties or specific external disturbances, the robust servomechanism is a tracking controller that can track broad reference signals asymptotically. For usage in the LQR state feedback law, the whole state is estimated using a Leuenberger observer.

3.1. Full state feedback design

The full-state-feedback controller is constructed, and a step reference is monitored through robust servomechanism design. Since actuator state feedback is unavailable, it is not included in the design model.

The design model formulation is as follows:

$$\begin{bmatrix} \dot{e} \\ \dot{\xi} \end{bmatrix} = \begin{bmatrix} 0 & C_{Az} \\ 0 & A \end{bmatrix} \begin{bmatrix} e \\ \xi \end{bmatrix} + \begin{bmatrix} D_{Az} \\ B \end{bmatrix} \mu \tag{14}$$

Where ξ is $\dot{x}$, μ is $\dot{U}$ and e is $Az - Az_{\text{reg}}$ Comparing the above equation with

$$\dot{z} = \tilde{A}z + \tilde{B}\mu \tag{15}$$

One uses the $\tilde{A}$ and $\tilde{B}$ matrices above in Matlab's "lqr" solver and gets the gains. Those gains regulate the above plant. Those gains are used to formulate our control law as follows.

$$U = -K_{ei} \int (Az - Az_{reg}) - K_\alpha \alpha - K_q q \tag{16}$$

After realizing the gains, design the analysis model, incorporating actuator dynamics, and produce the closed-loop model to monitor the reference. The lack of consideration for actuator dynamics in calculating the gain may result in deviation from the ideal LQR properties. However, the integrator will still allow for asymptotic tracking of the reference. Creating design charts for design parameters was necessary, which involved evaluating a range of penalty values for the (e_I) term in the design model. This helps in deciding the design point and allows us to develop more intuition about the effects of penalties.

3.2. Dynamic compensator with observer

The design of an observer was performed using the extended design model dynamics:

$$\begin{bmatrix} \dot{e}_I^{Az} \\ \dot{\alpha} \\ \dot{q} \end{bmatrix} = \begin{bmatrix} 0 & C_{\text{sp}}^{Az} \\ 0 & A_p \end{bmatrix} \begin{bmatrix} e_I^{Az} \\ \alpha \\ q \end{bmatrix} + \begin{bmatrix} D_{\text{sp}}^{Az} \\ B_p \end{bmatrix} U + \begin{bmatrix} -1 \\ 0 \\ 0 \end{bmatrix} ref \tag{17}$$

$$y = \begin{bmatrix} 1 & 0 & 0 \\ 0 & 0 & 1 \end{bmatrix} \begin{bmatrix} e_I^{Az} \\ \alpha \\ q \end{bmatrix} \tag{18}$$

where: $\dot{e}_I^{Az}$ is the rate of change of angle of attack error in the inertial frame, $\dot{\alpha} \ and \ \dot{q}$ is the rate of change of angle of attack and pitch rate respectively, U is the control input, ref is the reference input, A_p is the pitch damping coefficient, B_p is the control effectiveness coefficient for pitch rate, C_{sp}^{Az} is the static stability coefficient for angle of attack, D_{sp}^{Az} is the control effectiveness coefficient for angle of attack in the Short Period dynamics of the missile.

$$\tilde{A} = \begin{bmatrix} 0 & C_{sp}^{Az} \\ 0 & A_{sp} \end{bmatrix}$$
$$\tilde{B} = \begin{bmatrix} D_{sp}^{Az} \\ B_{sp} \end{bmatrix} \tag{19}$$
$$\tilde{C} = \begin{bmatrix} 1 & 0 & 0 \\ 0 & 0 & 1 \end{bmatrix}$$

The design process utilizes the property of duality between controllability and observability by employing the $\tilde{A}^T$ and $\tilde{C}^T$ in the LQR solver in MATLAB to obtain the L gains. [14].

3.3. Integrating the Autopilot with Guidance

The Autopilot takes $A_{z_{cmd}}$ as the input and creates A_z (the actual vertical acceleration). A_z is fed in as the acceleration of the Missile perpendicular to the LOS vector into the ProNav dynamics. The ProNav Guidance law, in turn, generates $A_{z_{cmd}}$ based on the current positions and velocities of the missile and the target.

An assumption made: It should be noted that A_z is assumed to be aligned with the perpendicular to the LOS direction of the guidance problem. This assumption, that A_z is the vertical acceleration in the inertial frame, only makes sense when dealing with modest LOS angles.
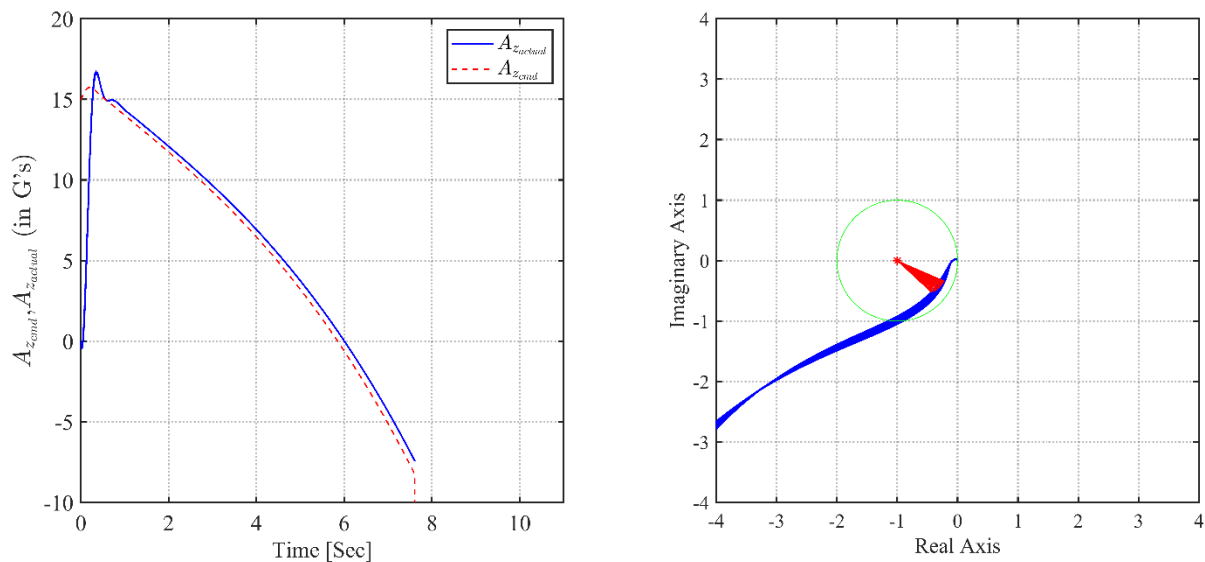

Figure 2. Output FB - Observer Design $A_{z_{cmd}}$ tracking and Nyquist iterates through test values of ρ

The analysis of the design requirements and the contribution of the e_I conviction to each of them is given prior. It can be simplified that increasing the penalty results in higher LQR gains, leading to an improvement in closed-loop response, but it also affects robustness. Hence, the robustness and the quality of time domain responses are critical factors that distinguish the system.

4. Simulation and Results

The control gains are computed using LQR with full-state feedback assumption. The LQR penalties are tuned to control the closed-loop system's time and frequency response characteristics. The system's performance is evaluated through simulations and plotted onto design charts to identify the best design that satisfies the requirements with a 10% safety margin. The tuning process is automated using MATLAB code to select the best design.

The Observer Gain Matrix is calculated by applying the LQR method to the Observer Design Model Matrices. The equation determines the penalties for LQR:

$$Q_e = Q_o + \frac{1}{\rho}\left(\tilde{B}\tilde{B}^T\right) \tag{20}$$

The equation provided is the formula for the augmented covariance matrix Q_e used in the LTR design method, hence Q_o is the initial covariance matrix and ρ is a scaling parameter that controls the trade-off between the input and output error. The term $\frac{1}{\rho}\left(\tilde{B}\tilde{B}^T\right)$ is added to increase the penalty on the control input, $\tilde{B}$ is the matrix relating the input to the output error, and B is the input matrix. In (20), Q_o is chosen to be a 3x3 identity matrix, and ρ is varied logarithmically between 1 and 0.01 (corresponding to log space (0,-2,30) in MATLAB), indicating a range of LTR parameter values. Lower values of ρ lead to higher control effort penalties, resulting in better loop recovery. However, it is important to ensure that the penalty is not too low, or the closed-loop poles may not meet the design requirements.
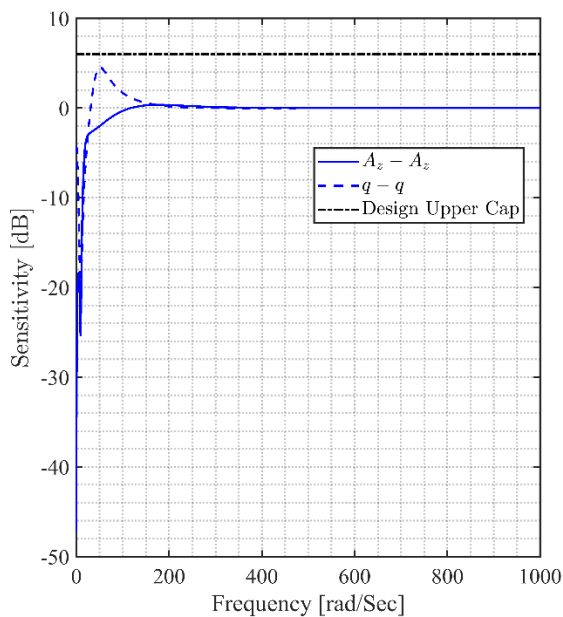

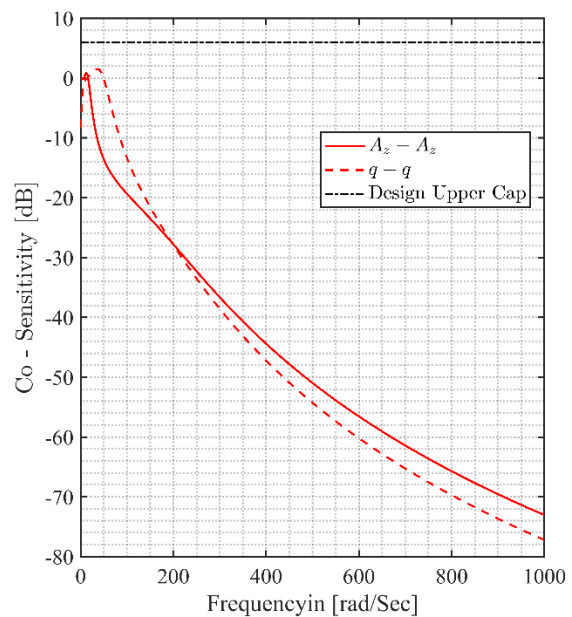**Figure 3.** Sensitivity Vs Frequency for final design

Figure 4. Co-sensitivity Vs Frequency for final design

4.1. Interception scenario

At the height of 42,000 feet, the target is detected by the operator. The target is flying at 400 ft/s with a flight path angle equal to zero, directly overhead the manned aircraft and aiming the nose on the x-axis of the target body coordinate system. Missile is launched from its carrier with a heading error of -20 degrees. After launching the missile, the target performs an avoidance 3 g accelerating maneuver that is orthogonal on its course. Proportional navigation law has the potential to simulate the scenario mentioned above, integrating the pursuer autopilot into the guidance loop and establishing the lowest miss distance to the target. However, the missile's structural limitations only accommodate an acceleration of up to 21g.

Table 1.The values for the computation of the state space model

Parameter	Value		Parameter	Value
Z_α	$A_{sp}(1,1) * V_0$		V_M	856.499 m/Sec
M_α	$A_{sp}(2,1)$		V_T	100 m/Sec
M_q	$A_{sp}(2,2)$		g	9.81
Z_{δ_e}	$B_{sp}(1,1) * V_0$		ζ_a	0.71
M_{δ_e}	$B_{sp}(2,1)$		C_{sp}^{Az}	$[Z_\alpha, 0]$
ω_a	35*2*pi		D_{sp}^{Az}	Z_{δ_e}
ρ	0.4454		D_a	0

The following steps demonstrated the design and implementation of a control system that meets the specified requirements, as shown in figures 2, 3, and 4.

Defining the open loop plant and extracting its short period dynamics, defining the actuator state space model, performing a full state feedback analysis iterating over different penalty values to find the optimal design point, and creating design charts.

Subsequently, designing an observer and identifying necessary matrices for finding observer gains, identifying the design point through gain crossover frequency, defining a dynamic compensator and pre-allocating design parameters, closing the loop with the actuator and compensator, collecting sensitivity and co-sensitivity data, finding the loop gain and creating design charts.
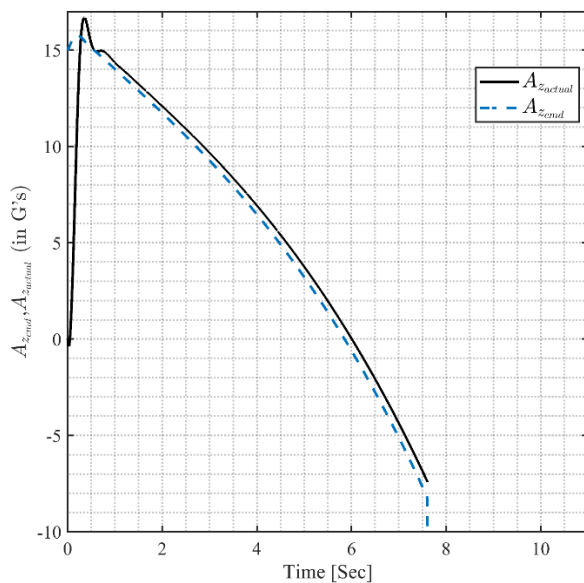

Figure 5. Tracking of $A_{z_{cmd}}$ by Missile's $A_{z_{actual}}$ final design
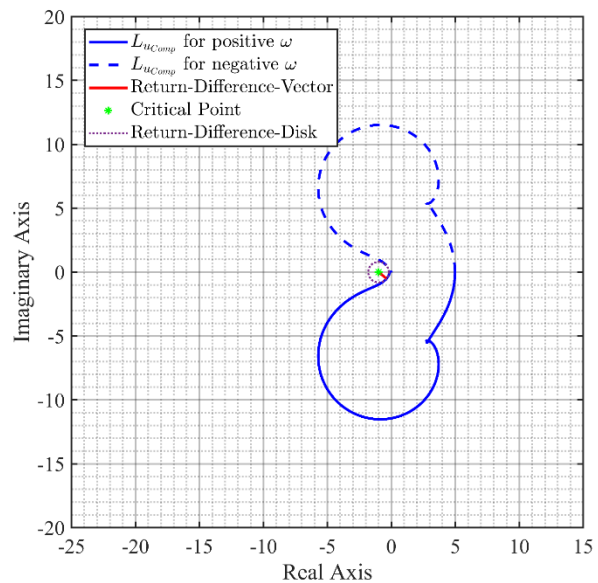

Figure 6. Observer design Nyquist plot

Then, plotting the design point's response and showing that design parameters are met, collecting step response data, finding the loop gain, integrating the guidance for the design point, and defining the closed-loop matrices. Table 1 from the designed plant provides the values for some variables.

The stability of the closed-loop system is determined by the number of encirclements of the critical point (-1+0j) in the Nyquist plot figure 6. A closed-loop system is considered stable if the Nyquist plot has zero encirclements of the critical point. The "margin" command in MATLAB gives the phase margin, but it may not be the gain margin critical to stability if the Nyquist plot has multiple phase cross-over frequencies. In this case, a custom algorithm should determine the gain margin that impacts stability [15].
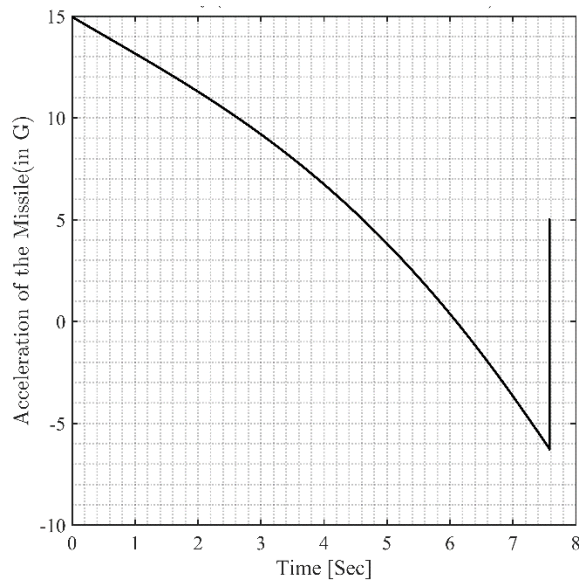
Figure 7. A_z of the missile with 3g target maneuver
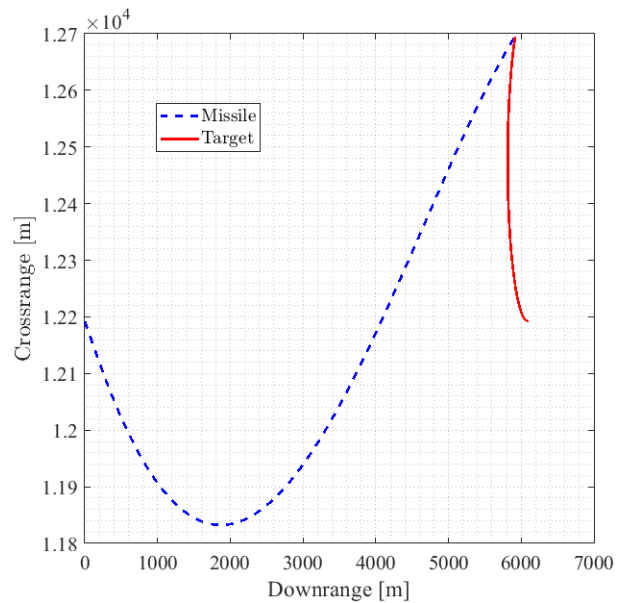

Figure 8. Missile Target engagement scenario with 0.006 m miss distance

4.2. Result analysis

Dutch Roll mode is represented by$(-1.2895 + 21.8316i, -1.2895 - 21.8316i)$, Short Period mode is represented in $(-1.0795 + 9.0780i, -1.0795 - 9.0780i))$, and Roll Subsidence mode is represented by (0.5815), the true pole.

The Dutch Roll Mode (highest negative real component of poles) is the fastest for the system in operation, indicating oscillations in the rolling-yawing motion dissipate more quickly than oscillations in the longitudinal motion (i.e., A.O.A and Pitch Rate: Short Period Mode) [16].
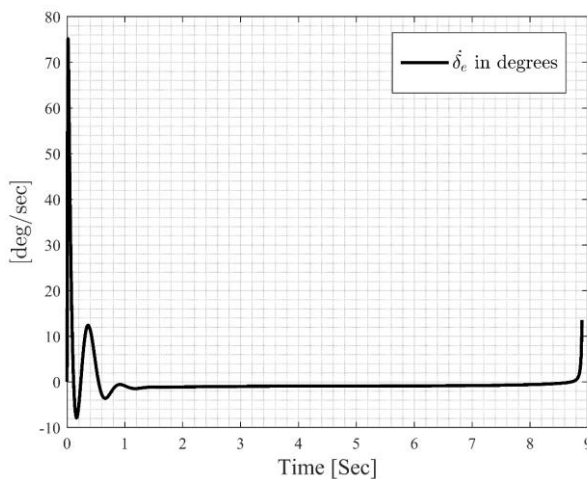

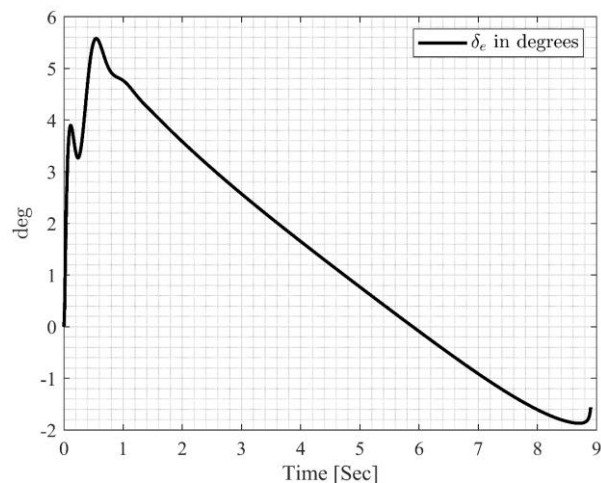**Figure 9.** Elevator deflection rate of change

Figure 10. Elevator deflection excitation

The three modes are all steady; the poles of the extracted short-period dynamics state-space model$(A_{sp}, B_{sp}, C_{sp}, D_{sp})$ are almost the same as the poles of the original short period mode and are as follows: $\begin{bmatrix} -1.0800 + 9.0843i \\ -1.0800 - 9.0843i \end{bmatrix}$.
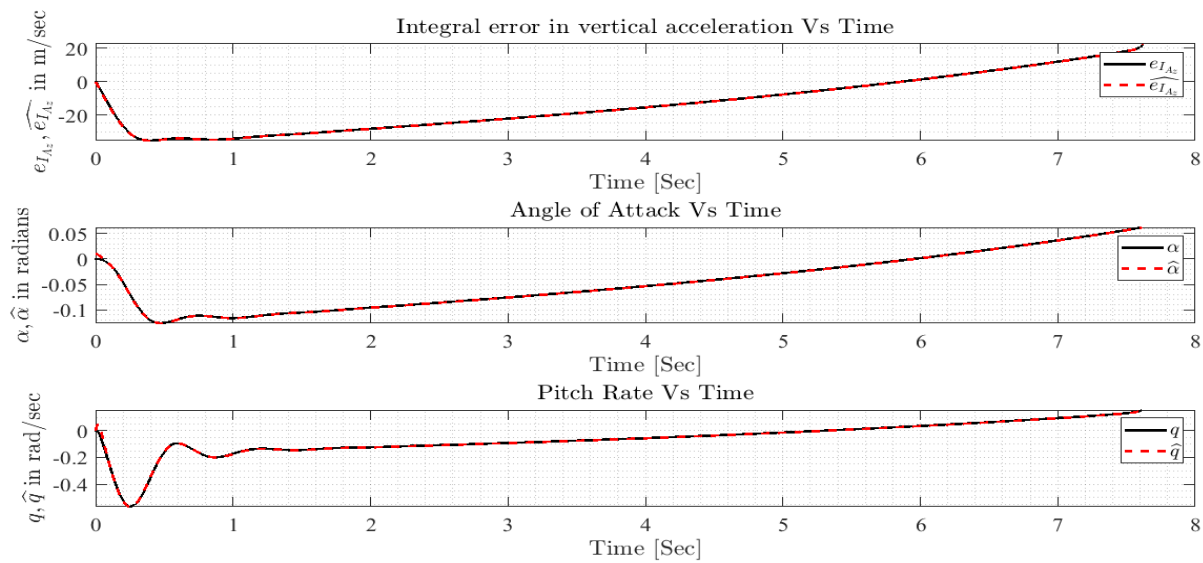
Figure 11. Observer estimates tracking actual states and integral error in longitudinal dynamics

In this study, the scalar-weighting factor utilized in the LQR design, the parameter R_LQR is set to one. The design also utilized Pro-Nav parameters, set ($n_P = 3.5$), equal to 3 times 9.81, for evasive maneuver was defined as a 3g acceleration normal to the velocity vector, with a heading error of -20 degrees in radians as shown in figures 5,7, and 8. The design of the control system utilized these parameters to ensure that the specified requirements are met and the desired performance is achieved. This is demonstrated by analyzing the deflection excitation and its rate figures 9, 10 that can quickly resolve the missile actuator by tracking actual states and integral error in magnificent track as in figure 11.

After introducing the observer in the design process, the values of the design factors need to be adjusted. While the full-state-feedback closed-loop system's behavior can be restored using LTR, increasing the observer gains is not recommended to maintain the same stability and performance specifications as it could lead to other problems, such as increased sensor noise. To ensure that the control system meets the desired performance and specified requirements, the LQR is tuned with a great approach to satisfy each design criterion with a 10 percent safety margin of the original design criteria using an integral cost function. This tuning process avoids over-tuning the observer gains, which could provoke drawbacks such as boosting sensor noise. The deflection excitation and its rate demonstrate the desired performance of the control system designed using these parameters.

5. Conclusion

Designing a longitudinal autopilot system for flying vehicles is crucial to enhancing stability and improving control in unpredictable situations. The use of state-space formulation and integration of the LQR method, a Luenberger observer, and proportional navigation algorithms have shown promising results in compensating for in-flight disturbances and noise. The numerical simulations demonstrated a decrease in miss distance, highlighting the effectiveness and robustness of the autopilot system; hence, implementation in practical applications is recommended. Future work could involve testing and optimizing the system in a real-life environment to validate its performance. Additionally, integrating other advanced control techniques, such as model predictive control, could further enhance the system's capabilities. The versatility and robustness of LQR optimization methods in changing environments make them valuable tools for future advancements in the aviation industry.

References

[1]   Luo, F., Zhang, J., Lyu, P., Liu, Z & Tang, W. (2022). Carrier-based aircraft precision landing using direct lift control based on incremental nonlinear dynamic inversion. *IEEE Access* vol.**10**, pp. 55709–55725.

[2]   Fu, Z., Dai, Y., & Zhang, K. (2017). Research progress on design methods for missile integrated guidance and control. Proceedings of the 2017 International Conference on Automation, *Control and Robots*.

[3]   Ashraf, M., Safwat, E., M.Kamel, A., & Abozied, M. A. H. (2022). Design and analysis of a nonlinear flight control law based on extended state observer. *2022 International Telecommunications Conference (ITC-Egypt), IEEE.*

[4]   Dinesh, K., D, N., Vijaychandra, J., SeshaSai, B., Vedaprakash, K., & Srinivasa Rao, K. (2021). A review on cascaded linear quadratic regulator control of roll autopilot missile. *SSRN Electronic Journal.*

[5]   Kumare, V., & Jerome, J. (2016). Algebraic Riccati equation based Q and R matrices selection algorithm for optimal LQR applied to tracking control of 3rd order magnetic levitation system. *Archives of Electrical Engineering*, vol.**65 (1)**, pp.51–169.

[6]   Bużantowicz, W. (2020). A sliding mode controller design for a missile autopilot system. *Journal of Theoretical and Applied Mechanics*, vol.**58 (1)**, pp.169–182.

[7]   Elumalai, V. K., & Subramanian, R. G. (2017). A new algebraic LQR weight selection algorithm for tracking control of 2 DoF torsion system. *Archives of Electrical Engineering*, vol.**66 (1)**, pp.55–75.

[8]   Holzhüter, T. (1997). LQG approach for the high-precision track control of ships. *IEE Proceedings-Control Theory and Applications*, vol.**144 (2)**, pp.121–127.

[9]   Chatys, R., Panich, A., Jurecki, R. S., & Kleinhofs, M. (2018, April). Composite materials having a layer structure of "sandwich" construction as above used in car safety bumpers. *In 2018 XI International Science-Technical Conference Automotive Safety. IEEE.*

[10] Nocoń, Ł., Grzyb, M., Szmidt, P., Koruba, Z., & Nowakowski, Ł. (2022). Control analysis with modified LQR method of anti-tank missile with vectorization of the rocket engine thrust. *Energies,* vol.**15 (1)**, pp.356.

[11] Safwat, E., Abozied, M. A., & Kamel, A. (2021). Design and analysis of a nonlinear guidance law for small UAV. *In AIAA Scitech 2021 Forum.*

[12] Chen, K., Fu, B., Ding, Y., & Yan, J. (2015). Integrated guidance and control method for the interception of maneuvering hypersonic vehicle based on high order sliding mode approach. *Mathematical Problems in Engineering*, vol.**2015**, pp.1–19.

[13] Arikapalli, V. M., Bhowmick, S., Rao, P. B., & Ayyagari, R. (2022). Investigative design of missile longitudinal dynamics using LQR-LQG controller in presence of measurement noise and inaccurate model. *Sādhanā*, vol.**47 (1)**.

[14] Kim, T., Shim, H., & Cho, D. D. (2016, December). Distributed Luenberger observer design. *In 2016 IEEE 55th Conference on Decision and Control (CDC)* (pp. 6928 6933). *IEEE.*

[15] Jia, Q., Hu, J., Safwat, E., & Kamel, A. (2021). Polar coordinate system to solve an uncertain linguistic Z-number and its application in multicriteria group decision making. *Engineering Applications of Artificial Intelligence*, vol.**105**, pp.104437.

[16] Wang, B., Liu, D., Wang, W., & Peng, X. (2018). A hybrid approach for UAV flight data estimation and prediction based on flight mode recognition. *Microelectronics Reliability*, vol.**84**, pp.253-262.